Vascular Dynamics of Cerebral Gliomas Investigated with Selective Catheter Angiography, Perfusion CT and MRI

Roland Wiest[1], Ralph Schaer[1], Michael H. Reinert[2], Ferdinand H. von Bredow[1], Marwan M. El Koussy[1], Luca Remonda[1], Gerhard Schroth[1], Christoph Ozdoba[1], Johannes Slotboom[1]

Abstract

Purpose: To assess if intratumoral blood circulation parameters from dynamic susceptibility contrast (DSC) MRI and dynamic CT deliver comparable results and to compare tumor-related changes in regional cerebral blood flow (rCBF) and regional cerebral blood volume (rCBV) with arterial, intratumoral, and venous transition detected with digital subtraction angiography (DSA).

Patients and Methods: Ten patients with cerebral gliomas were prospectively studied with DSC-MRI, dynamic CT and DSA. Tumor areas were segmented and perfusion maps for rCBF, rCBV, and mean transit time (MTT) were computed from DSC-MRI and dynamic CT. Arterial circulation time (ACT), intermediate circulation time (ICT), and venous appearance time (VAT) were measured with DSA. Asymmetry indices (AIs) were calculated for MRI- and CT-based perfusion values, for ICT and VAT and compared among each other.

Results: DSC-MRI and dynamic CT yielded comparable AI values for rCBF (MRI: 39.5 ± 20.4, CT: 36.0 ± 17.9, Pearson's correlation $r^2 = 0.91$) and rCBV (MRI: 44.6 ± 20.9 vs. CT: 40.9 ± 16.3, $r^2 = 0.84$). The MTT AI (MRI: –4.7 ± 11.2 vs. CT: –0.5 ± 10.4, $r^2 = 0.47$) showed only a weak correlation. ICT correlated with rCBV (ICT: 38.4 ± 14.7, $r^2 = 0.59$, and dynamic CT: $r^2 = 0.81$) and VAT with rCBF (VAT: 31.7 ± 17.6, $r^2 = 0.73$, and dynamic CT: $r^2 = 0.87$), but not with MTT.

Conclusion: CT and MRI methods provide consistent information about tumor vascularity of cerebral gliomas in accordance with DSA.

Key Words: Perfusion CT · MRI · Angiography · Glioma · Grading

Clin Neuroradiol 2008;18:98–106
DOI 10.1007/s00062-008-8011-y

Durchblutung zerebraler Gliome. Eine Studie mit DSA, Perfusions-CT und MRT

Zusammenfassung

Ziel: Vergleichsstudie zur Perfusionsmessung mittels CT- und MR-Perfusion bei Hirntumoren mit der Fragestellung, inwieweit beide Schnittbildverfahren bezüglich der Parameter regionaler zerebraler Blufluss (rCBF), regionales zerebrales Blutvolumen (rCBV) und mittlere Transitzeit (MTT) vergleichbare Ergebnisse zeigen. Die Ergebnisse werden mit den dynamischen Untersuchungsergebnissen der digitalen Subtraktionsangiographie (DSA) verglichen.

Patienten und Methodik: Zehn Patienten mit hirneigenen Tumoren wurden prospektiv mittels MR-Perfusion, CT-Perfusion und DSA untersucht. Die Tumoren wurden segmentiert. In den segmentierten Arealen wurden rCBF, rCBV und MTT aus den Daten beider Modalitäten berechnet. Die arterielle Zirkulationszeit (ACT), intermediäre Zirkulationszeit (ICT) und venöse Anflutungszeit (VAT) wurden mittels DSA bestimmt. Regionenbasierte Asymmetrieindizes wurden für die CT- und MR-Perfusion, für ICT und VAT berechnet und verglichen.

Ergebnisse: MR- und CT-Perfusion lieferten vergleichbare Ergebnisse für rCBF (MRT: 39,5 ± 20,4, CT: 36,0 ± 17,9, Pearson-Korrelation $r^2 = 0,91$) und rCBV (MRT: 44,6 ± 20,9 vs. CT: 40,9 ± 16,3, $r^2 = 0,84$). Der Asymmetrieindex für MTT (MRT: –4,7 ±

[1]Institute of Diagnostic and Interventional Neuroradiology, Inselspital, University of Bern, Switzerland,
[2]Department of Neurosurgery, Inselspital, University of Bern, Switzerland.

Received: November 12, 2007; revision accepted: February 4, 2008

11,2 vs. CT: –0,5 ± 10,4, r^2 = 0,47) zeigte lediglich eine schwache Korrelation zwischen den Modalitäten. Die ICT korrelierte mit dem rCBV (ICT: 38,4 ± 14,7, r^2 = 0,59, CT: r^2 = 0,81) und die VAT mit dem CBF (VAT: 31,7 ± 17,6, r^2 = 0,73, CT: r^2 = 0,87), jedoch nicht mit der MTT.

Schlussfolgerung: Die Perfusionsmessung intrazerebraler Tumoren mittels CT und MRT liefert vergleichbare Ergebnisse, auch in Übereinstimmung mit der DSA.

Schlüsselwörter: Perfusions-CT · MRT · Angiographie · Gliom · Grading

Introduction

In clinical practice, computed tomography (CT) and magnetic resonance imaging (MRI) are the investigations of choice in the evaluation of brain tumors [1–3]. Angiographic techniques for the detection of neovascularity or arteriovenous shunting [4] and brain perfusion techniques like dynamic susceptibility contrast-(DSC-) MRI and dynamic CT may assist in distinguishing high-grade from low-grade tumors [5, 6]. The detection of early opacification of a tumor-draining vein and the dynamics of tumor hypervascularity are still useful observations to determine tumor grading without biopsy, especially when the tumor is located in an eloquent region of the brain. Several studies have demonstrated the correlation between microvessel density and increased relative cerebral blood volume in high-grade tumors with DSC-MRI [7–10]. To a lesser extent, the dynamic CT approach has been used in animal models and clinical practice [11, 12]. Yet, only few studies have focused on the comparability and reproducibility of different brain perfusion techniques in brain tumor imaging [13]. The routine use of CT in initial neuroradiologic diagnostics as well as its widespread clinical availability make dynamic CT a useful method to generate parametric maps of regional cerebral blood flow (rCBF) and regional cerebral blood volume (rCBV) for tumor grading.

The calculation of rCBF and rCBV according to the indicator-dilution theory [14], which is the basis of most commercially available software programs today, is limited due to the disruption of the blood-brain barrier and may lead to an overestimation of CBF and CBV. Beyond complex calculations of fractional plasma volume and vascular transfer constant [15], digital subtraction angiography (DSA) offers the advantage of directly investigating the increased tissue perfusion and its influence on intratumoral blood velocity with a high temporal and spatial resolution method. Comparative studies, however, which investigate the vascularity of cerebral gliomas with different parametric imaging techniques and DSA, do not exist. The purpose of the study was to test if (1) intratumoral blood circulation parameters are comparable between DSC-MRI and dynamic CT in a single-compartment model, and (2) if tumor-related relative changes of rCBF and rCBV in DSC-MRI and dynamic CT match the arterial, intratumoral and venous transition as determined from DSA.

Patients and Methods

Patients

Ten patients, five women and five men, aged between 44 and 78 years (mean age 57.1 years), with suspected gliomas, as detected with conventional MRI (Table 1), were prospectively studied with DSC-MRI, dynamic CT and DSA. Informed consent was obtained from every patient according to the rules of the local ethics committee. All patients had clinical findings suggestive either of increased intracranial pressure or a focal neurologic deficit. All patients underwent DSC-MRI and dynamic CT on the same day. DSA was performed on the following day in all patients. Histological grading using stereotaxy or open tumor resection was done in seven patients. Two patients were histologically diagnosed with oligodendroglioma (WHO grade II and III), one patient with anaplastic astrocytoma (WHO grade III), and four patients with glioblastoma (WHO grade IV). Yet another three patients were diagnosed with glioblastoma (WHO grade IV) based on MRI findings, the detection of an early tumor-draining vein with DSA, and clinical and MRI follow-up. Histological confirmation was not obtainable in these cases due to unresectable tumors located in eloquent areas of the brain where even stereotactic biopsy was considered to be associated with an intolerable risk of periprocedural complications. These patients were treated with combined irradiation and chemotherapy. Although tumor grading is based on pathohistological evaluation, the combination of MRI and DSA has been used to approximate tumor grade of gliomas for many years [16].

Table 1. Clinical data and regional asymmetries for rCBF, rCBV, VAT, and ICT (from DSC-MRI, dynamic CT and DSA). CT: computed tomography; DSA: digital subtraction angiography; DSC: dynamic susceptibility contrast; F: female; ICT: intermediate circulation time; M: male; MRI: magnetic resonance imaging; rCBF: regional cerebral blood flow; rCBV: regional cerebral blood volume; VAT: venous appearance time; WHO: World Health Organization.

Patient #	Sex	Age (years)	WHO grade	Tumor site	MTT MRI	MTT CT	rCBF MRI	rCBF CT	rCBV MRI	rCBV CT	VAT DSA	ICT DSA
1	F	58	II	Left parietal lobe	3.5	–1.1	7.3	10.7	9.8	7.2	4.8	11.1
2	F	78	III	Right paracentral lobe	–20.8	–4.3	48.1	38.1	29.6	35.9	20.0	27.3
3	M	44	III	Right frontal lobe	–13.5	–4.56	12.9	15.8	38.1	35.4	15.8	33.3
4	F	69	IV	Right frontal and parietal lobe	–6.03	3.62	18.3	16.7	34.3	23.4	23.1	33.3
5	M	44	IV	Biparietal	2.87	–7.2	41.0	23.1	21.9	40.3	11.1	45.0
6	F	70	IV	Right parietal and occipital lobe	–16.78	8.6	42.9	42.9	59.1	58.5	52.9	45.5
7	M	64	IV	Left frontal and parietal lobe	–3.69	–1.5	45.4	46.7	55.5	45.8	50.0	33.3
8	M	44	IV	Left frontal lobe	4.14	13.7	51.9	52.9	59.1	55.5	42.9	42.9
9	M	53	IV	Left temporal lobe	12.69	10.0	56.3	60.0	63.6	57.9	46.7	66.7
10	F	47	IV	Right temporal	–18.2	–22.5	70.8	52.7	75.2	49.2	50.0	40.0

During follow-up of the patient cohort, both patients with suspected grade II did not show any signs of dedifferentiation up to now. All patients who presented with suspected grade IV glioma died from their brain tumor within 1 year after the MRI, CT, and DSA studies, thus further supporting the suspected diagnosis post hoc. The classification and grading applied in this study are based on the current WHO classification of nervous system tumors [17].

MR and CT Image Acquisition

MRI was performed on a 1.5-T Siemens Sonata system (Siemens Medical Systems, Erlangen, Germany). A dynamic series was performed after bolus injection of 10 ml Gadovist® 1.0 (Bayer Schering Pharma, Baar, Switzerland) acquiring 40 images in twelve adjacent slices using an adapted 2-D echoplanar imaging sequence (slice thickness 5 mm; TR 1.44 s, TE 47 ms; FA 90°, FOV 230 × 230 mm, matrix 128 × 128 interpolated to 256 × 256 for postprocessing). Total acquisition time was 80 s. The CT studies were performed on a GE Light-speed QX/I 8 slice multislice scanner (General Electric, Milwaukee, WI, USA). A dynamic contrast-enhanced cine scan (80 kV, 200 mA) was performed after bolus injection of 40 ml of a high-iodine-concentration nonionic contrast agent (Iomeron® 400, Bracco SA, Milan, Italy) with an iodine concentration of 400 mg/ml, as reported previously [18]. The studies were acquired in two adjacent 10-mm sections with a temporal resolution of 1 s over a period of 45 s.

Angiography

DSA was performed on a biplane angiographic X-ray system (Toshiba KXO-80C & 80D with a Toshiba DFP 2000/A image processing unit, Tokyo, Japan) by the same investigator. DSA images were acquired in standard (anteroposterior and lateral view) and oblique projections with a time resolution of 0.4 s. Image matrix was 1,024 × 1,024 with a 12" image intensifier. No complications during or after (in relation to) DSA were reported.

Intraarterial four-vessel selective DSA was performed in local anesthesia over conventional 6-F sheaths (Terumo Corp., Tokyo, Japan) via the right or left femoral artery with dedicated 5.5-F catheters (Cook JB-2, Bjaevrskov, Denmark). Selective DSA (83–86 kV, 125 mA) was performed by selective injections of a nonionic contrast agent (Iopamiro® 300, Bracco SAy) into both common carotid and vertebral arteries at a flow rate of 5 ml/s.

Postprocessing and Analysis of Scans

The parameter maps used for the assessment of cerebral hemodynamics included rCBF, rCBV, and mean transit time (MTT). These were calculated according to the indicator-dilution model for both imaging modalities [19]. The parameter maps were computed for both DSC-MRI and dynamic CT with an in-house developed application written in JAVA-2 that uses a singular value decomposition-(SVD-)based algorithm [20]. The application was specifically developed to handle perfusion imaging data of both imaging modalities.

Regions of interest (ROIs) in the tumor were then segmented semiautomatically from rCBF, rCBV and MTT maps, including solely regions with increased intensity thresholds. For DSC-MRI and dynamic CT evaluation, two ROIs were placed semiautomatically in a corresponding scan for rCBF, rCBV, and MTT. The first ROI was drawn to mark the tumor outline, excluding the necrotic core in highly malignant gliomas. The second ROI of similar volume as the first was applied contralaterally into the nonaffected white matter through a mirroring function with manual correction (Figure 1). In cases where the neoplasm involved both hemispheres of the brain and mirroring to the corresponding contralateral region was not possible, regions of comparable perfusion values within healthy tissue in the frontal or parietal lobe were used for internal reference. In order to compare the individual perfusion maps in different vascular areas for every patient, a relative cerebral transit time, blood flow and volume ratio was calculated from all mean DSC-MRI and dynamic CT-based perfusion values. Since we do not have the possibility to absolutely quantify CT and MR perfusion values, we have chosen to use the asymmetry index (AI) to compare both methods. The methodological advantage of using these indices is that they are inherently independent of specific machines, protocols, or contrast kinetics [21, 22]. Arterial, parenchymal, and venous phases in DSA were estimated from direct inspection of the high-resolution DSA images on a PACS workstation (Figures 2a and 2b). The transit time between the monitored points was calculated with a temporal resolution of 0.4 s (2.5 frames/s) as follows: arterial circulation time (ACT) from the start of arterial filling of the cavernous part of the internal carotid artery to the time the terminal arterial branches were opacified, intermediate circulation time (ICT) from the end of the arterial filling to the beginning of the venous phase, and venous appearance time (VAT) from maximum arterial opacification to the appearance of contrast medium in the cortical veins [23]. Separate calculations were performed for the unaffected hemisphere, the affected hemisphere and the tumor region itself. These parameters were directly compared between the middle cerebral arteries (MCA) of the left and right

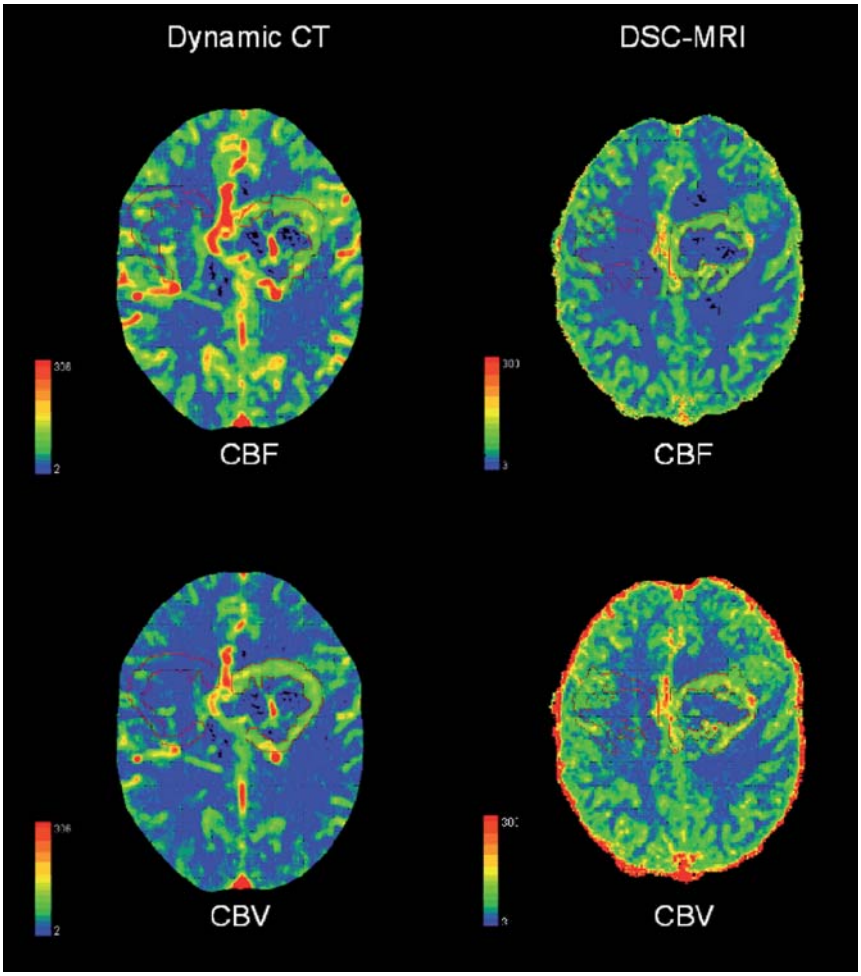

Figure 1. Parametric perfusion maps of patient # 7. Increased rCBF and rCBV are observed in both DSC-MRI and dynamic CT. According to the higher spatial resolution of the dynamic CT images, the hyperperfused tumor rim is better resolved.

hemisphere if the tumor did not cross the hemisphere, and between the anterior (ACA) and middle cerebral arteries if the tumor crossed the midline. Furthermore, intratumoral arterial, parenchymal, and venous opacification times as defined above were compared with the respective parameters in the contralateral hemisphere. To compare the time course of the angiogram with the results of the parametric perfusion maps from DSC-MRI and dynamic CT, a relative AI [(affected – unaffected region)/(affected + unaffected region)*100] was calculated for every parameter.

Three board-certified neuroradiologists blinded to the histological results reviewed and discussed all DSC-MRI, dynamic CT and DSA studies until consensus was obtained. Statistical analysis included Student's two-tailed t-test for comparison of the perfusion-based pixel intensity values of DSC-MRI, dynamic CT and the circulation times of DSA. Pearson's correlation coefficients were calculated to test the correlation between the perfusion parameters obtained from the two imaging modalities and ACT, ICT, and VAT.

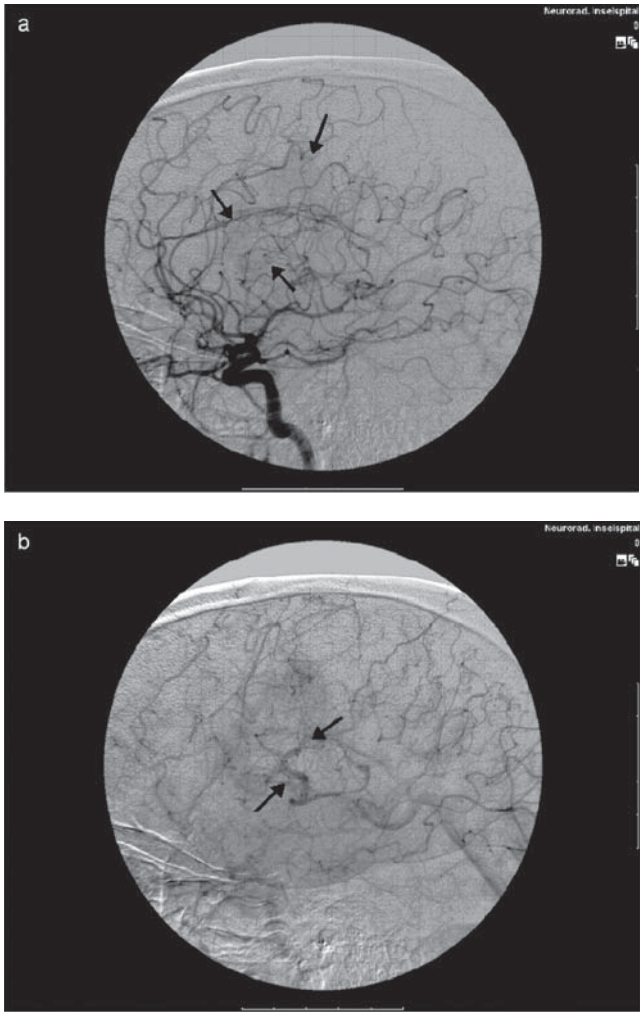

Figures 2a and 2b. The lateral view of the DSA shows the begin of the parenchymal phase (a, arrows) of the tumor and the early opacification of the venous drainage (b, arrows), indicating a neovascularized glioblastoma multiforme (patient # 7).

Results

Dynamics of MR versus CT Perfusion Studies

All ten patients received DSC-MRI and dynamic CT on the same day. There was an excellent correlation between the rCBF AI and rCBV AI values calculated from DSC-MRI and dynamic CT. In all cases, asymmetric perfusion was detected in DSC-MRI as well as in dynamic CT relative to normal white matter (Table 1). Perfusion imaging in one patient with a grade II tumor revealed only mild intratumoral hyperperfusion compared to contralateral white matter on DSC-MRI and dynamic CT. Excellent correspondence between DSC-MRI and dynamic CT was obtained from the rCBF maps (MRI: mean AI = 39.5, SD ± 20.4, CT: mean AI 36.0 ± 17.9, Pearson's correlation $r^2 = 0.91$). rCBV AI values were: MRI: 44.6 ± 20.9 versus CT: 40.9 ± 16.3, $r^2 = 0.84$. For the MTT AI (MRI: –4.7 ± 11.2 vs. CT: –0.5 ± 10.4, $r^2 = 0.47$), there was only a weak intermodality correlation.

Dynamics of DSA

All ten patients received DSA 1 day after DSC-MRI and dynamic CT. The intratumoral vessels of all patients showed increased tortuosity and increased microvascular density. Patients 4–10, who had grade IV gliomas, showed aberrant and early venous filling during the arterial phase of the angiogram. The ACT values did not show any relevant differences between the unaffected hemisphere and the tumor itself (p = not significant). ICT was significantly reduced in the capillary network of the tumor ($p < 0.0001$), and the extratumoral vessels of the affected hemisphere ($p = 0.001$). VAT showed an accelerated arteriovenous bolus passage in the affected hemisphere ($p = 0.0003$) and the tumor ($p = 0.002$), indicating an increased tumor flow rate (Table 2).

Correlations between DSC-MRI, Dynamic CT and DSA

Pearson's correlation coefficient was calculated for differences in the relative asymmetry of different perfusion parameters between the tumor region and the contralateral, unaffected hemisphere. To compare the values

Table 2. DSA-related hemodynamic parameters for the unaffected and affected hemisphere versus tumor. ACT: arterial circulation time; ICT: intermediate circulation time; VAT: venous appearance time.

Patient #	ACT (s) Unaffected	Affected	Tumor	ICT (s) Unaffected	Affected	Tumor	VAT (s) Unaffected	Affected	Tumor
1	2.0	2.0	1.6	2.0	2.0	1.6	4.4	4.4	4.0
2	1.6	1.6	1.6	2.8	2.0	1.6	6.0	6.0	4.0
3	1.6	2.0	2.8	2.4	2.4	1.2	4.4	4.8	3.2
4	1.2	1.2	2.0	1.6	0.8	0.8	3.2	2.4	2.0
5	1.2	1.2	1.2	3.2	3.2	1.2	6.0	4.8	4.8
6	1.2	1.2	1.6	3.2	2.8	1.2	5.2	4.8	1.6
7	1.2	1.6	1.2	2.4	2.8	1.2	4.8	5.2	1.6
8	1.2	1.6	1.6	2.0	2.0	0.8	4.0	3.6	1.6
9	1.6	1.6	1.2	2.0	1.2	0.4	4.4	3.6	1.6
10	1.6	2.0	0.4	2.8	2.0	1.2	4.8	5.6	1.6

ACT: unaffected vs. affected hemisphere $p = 0.25$; affected vs. tumor $p = 0.72$; unaffected vs. tumor $p = 0.71$. ICT: unaffected vs. affected hemisphere $p = 0.28$; affected vs. tumor $p < 0.0001$; unaffected vs. tumor $p = 0.001$. VAT: unaffected vs. affected hemisphere $p = 0.65$; affected vs. tumor $p = 0.0003$; unaffected vs. tumor $p = 0.002$

of the parametric DSC-MRI and dynamic CT maps with the temporal dynamics of tumor hypervascularity in DSA, an AI was calculated for ICT and VAT. Best correlation was achieved between ICT, an indicator for the vascular volume of the capillary network, and the parametric rCBV maps: ICT: 38.4 ± 14.7, DSC-MRI: 44.6 ± 20.9, Pearson's correlation $r^2 = 0.59$, and dynamic CT: 40.9 ± 16.3, Pearson's correlation $r^2 = 0.81$. The correlation between the duration of the arterial and capillary stain (VAT) and the parametric rCBF maps was: VAT: 31.7 ± 17.6, DSC-MRI: 39.5 ± 20.4, Pearson's correlation $r^2 = 0.73$, and dynamic CT 36.0 ± 17.9, Pearson's correlation $r^2 = 0.87$ (Table 3, Figure 3). There was, however, no correlation between MTT and ICT or VAT: ICT: 38.4 ± 14.7, DSC-MRI: –4.7 ± 11.6, Pearson's correlation $r^2 = 0.12$, and dynamic CT: –0.5 ± 10.4, Pearson's correlation $r^2 = 0.07$; VAT: 31.7 ± 17.6, DSC-MRI: –4.7 ± 11.6, Pearson's correlation $r^2 = 0.02$, and dynamic CT –0.5 ± 10.4, Pearson's correlation $r^2 = 0.12$ (Table 3, Figure 3).

Discussion

Derangements of the cerebral hemodynamics almost always occur in association with intracranial tumors. Such hemodynamic changes can be evaluated either by DSA or by parametric perfusion imaging techniques [24–26]. DSA is not generally used in the diagnostic work-up of brain tumors, some neurosurgeons, however, prefer to have information about a tumor's arterial supply, venous drainage, and compression of adjacent major intracranial vessels in high spatial resolution (< 200 µm), which can be achieved by catheter angiography only, to help them in planning an operative or stereotactic procedure. While DSC-MRI techniques have been widely used for clinical routine during the last few years, there is still limited use of dynamic CT because of its limitations regarding covered volume, exposition to ionizing radiation, and iodinated contrast agents. Compared to DSC-MRI, however, dynamic CT has shown advantages in the detection of tumor angiogenesis, according to the linear

Table 3. Mean AI ± SD and Pearson's correlations between DSC-MRI, dynamic CT, DSA ICT and DSA VAT. AI: asymmetry index; CBF: cerebral blood flow; CBV: cerebral blood volume; CT: computed tomgraphy; DSA: digital subtraction angiography; DSC: dynamic susceptibility contrast; ICT: intermediate circulation time; MRI: magnetic resonance imaging; MTT: mean transit time; SD: standard deviation; VAT: venous appearance time.

Modality	AI	Modality	AI	Pearson's correlation r^2
CBF DSC-MRI	39.5 ± 20.4	CBF dynamic CT	36.0 ± 17.9	0.91
MTT DSC-MRI	–4.7 ± 11.2	MTT dynamic CT	–0.5 ± 10.4	0.47
CBV DSC-MRI	44.6 ± 20.9	CBV dynamic CT	40.9 ± 16.3	0.84
DSA ICT	38.4 ± 14.7	CBV DSC-MRI	44.6 ± 20.9	0.59
DSA ICT	38.4 ± 14.7	CBV dynamic CT	40.9 ± 16.3	0.81
DSA VAT	31.7 ± 17.6	CBF DSC-MRI	39.5 ± 20.4	0.73
DSA VAT	31.7 ± 17.6	CBF dynamic CT	36.0 ± 17.9	0.87
DSA ICT	38.4 ± 14.7	MTT DSC-MRI	–4.7 ± 11.2	0.13
DSA ICT	38.4 ± 14.7	MTT dynamic CT	–0.5 ± 10.4	0.07
DSA VAT	31.7 ± 17.6	MTT DSC-MRI	–4.7 ± 11.2	0.02
DSA VAT	31.7 ± 17.5	MTT dynamic CT	–0.5 ± 10.4	0.12

relationship between contrast agent concentration and the CT attenuation coefficient, as well as to the absence of susceptibility artifacts [25]. Regarding the few studies and case series dealing with dynamic CT in the evaluation of brain tumors, the rCBF and rCBV patterns in our series were consistently delineating higher-grade gliomas. Furthermore, the rCBF and rCBV patterns were consistent between DSC-MRI and dynamic CT. In all ten patients, rCBF and rCBV were increased at the site of the tumor. Although a number of studies have shown increased rCBV values in tumors with increased microvascular density [8, 27–29], no reliable data exist on the reproducibility of repeated rCBV measurements. While most of the studies used manually placed similar rectangular or circular ROIs in the tumor to compare the attenuation values, we have chosen individually applicable polygonal ROIs, fitted to the individual extent of the hyperperfused tumor areas. With this approach, we have excluded necrotic regions and edema neighboring the angiogenetic tumor areas. Furthermore, we were able to apply approximately the same ROIs to the respective slices on dynamic CT and DSC-MRI to enable intermodal comparisons, which revealed strong correlations between both methods.

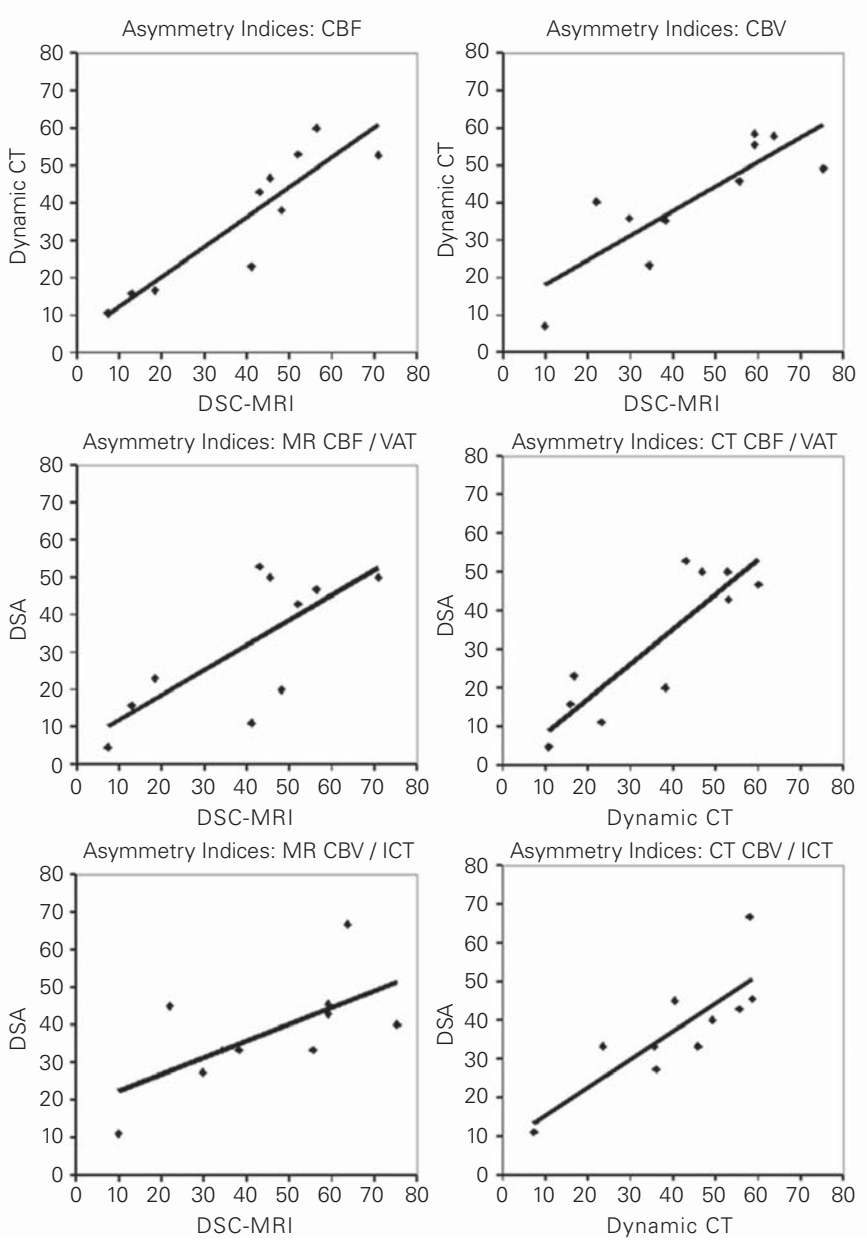

Figure 3. Correlations between DSC-MRI, dynamic CT, VAT and ICT. Best correlation is achieved for CBF between DSC-MRI and dynamic CT (r^2 = 0.91) and between DSA VAT and CBF in dynamic CT (r^2 = 0.87).

A comparison between parametric maps and angiographic findings is, by contrast, more difficult to achieve. Given the hypothesis of rCBV being the imaging analog of microvascular density [30], which is used in histopathologic evaluation, changes in the capillary passage time as measured with ICT should either indicate an increased tumor bed (prolonged ICT) or an early washout of the capillary stain (shortened ICT) by arteriovenous shunting, indicating tumor dedifferentiation. In our series, we found an accelerated ICT in the tumor in all patients. There was a strong correlation between ICT and rCBV in both DSC-MRI and dynamic CT. The cerebral blood flow is more complex to detect on DSA, and different attempts have been made to quantify rCBF with direct inspections of serial angiograms and time-density techniques. Some investigators have observed that arterial flow correlates well with the perfusion of the cerebral territory fed by that artery [31, 32]. As the angiographic cerebral circulation time has been shown to correlate with the fast component of CBF in healthy

volunteers and patients with stroke and subarachnoid hemorrhage [33], we have chosen the relative VAT as a parameter which best matches the filling of the arterial cerebral territory and capillary arteriovenous circulation together. In our series, we have found a shortened VAT at the site of the tumor compared to the contralateral hemisphere in all ten patients. For both DSA ICT and DSA VAT, the correlation with CT CBV and CT CBF, respectively, proved to be superior to the corresponding DSC-MRI values. This is most probably due to the fact that DSA and CT are closely related methods both using X-rays and iodinated contrast agents with linear concentration/contrast relationship.

MTT has been shown to correlate with the resistance of the distal vascular territory [34]. In our study, we found only a weak correlation between the parametric MTT maps of DSC-MRI and dynamic CT, and no relevant correlation with the angiographic circulation parameters.

For the MTT we observed AIs that are varying around zero from dynamic CT as well as from DSC-MRI measurements (Table 3). This means that the MTTs of the tumors examined in this study do, on average, not differ from healthy tissue. Since we examined only the nonnecrotic vital tumor parts, we must conclude that for this tissue type, the CBV as well as the CBF are increased in glioma while keeping their quotient, which is the MTT, approximately constant. We have found no relevant correlation between the parametric MTT maps of DSC-MRI and dynamic CT with ICT and VAT. Beyond the statistical drawback of a larger error in the computed estimation of the MTT AI, when grouped around zero, one has further to consider the large variance in the angiographic transition time, according to arteriovenous shunting [35] in high-grade gliomas. Therefore, MTT maps may provide equivocal results and are of little value in estimating the tumor grade [36].

Conclusion

This study compares DSC-MRI and dynamic CT perfusion parameters with angiographic findings in cerebral gliomas. Compared with digital angiography as a gold standard for the assessment of hemodynamics, the study shows that (1) the less invasive CT and MRI methods provide robust results while avoiding the drawbacks of angiography, and (2) perfusion CT, being cost effective and widely available, represents an attractive alternative to DSC-MRI for hemodynamic imaging of gliomas.

Conflict of Interest Statement

We certify that there is no actual or potential conflict of interest in relation to this article.

References

1. Kurki T, Lundbom N, Kalimo H, et al. MR classification of brain gliomas: value of magnetization transfer and conventional imaging. Magn Reson Imaging 1995;13:501–11.
2. Julia-Sape M, Acosta D, Majos C, et al. Comparison between neuroimaging classifications and histopathological diagnoses using an international multicenter brain tumor magnetic resonance imaging database. J Neurosurg 2006;105:6–14.
3. Earnest F, Baker HL Jr, Kispert DB, et al. Magnetic resonance imaging vs. computed tomography: advantages and disadvantages. Clin Neurosurg 1985;32:540–73.
4. Carmody RF, Seeger JF. Intracranial applications of digital subtraction angiography. Crit Rev Diagn Imaging 1984;23:1–40.
5. Choyke PL, Dwyer AJ, Knopp MV. Functional tumor imaging with dynamic contrast-enhanced magnetic resonance imaging. J Magn Reson Imaging 2003;17:509–20.
6. Wong JC, Provenzale JM, Petrella JR. Perfusion MR imaging of brain neoplasms. AJR Am J Roentgenol 2000;174:1147–57.
7. Law M, Oh S, Johnson G, et al. Perfusion magnetic resonance imaging predicts patient outcome as an adjunct to histopathology: a second reference standard in the surgical and nonsurgical treatment of low-grade gliomas. Neurosurgery 2006;58:1099–107.
8. Mills SJ, Patankar TA, Haroon HA, et al. Do cerebral blood volume and contrast transfer coefficient predict prognosis in human glioma? AJNR Am J Neuroradiol 2006;27:853–8.
9. Brasch RC, Li KC, Husband JE, et al. In vivo monitoring of tumor angiogenesis with MR imaging. Acad Radiol 2000;7:812–23.
10. Leach MO, Brindle KM, Evelhoch JL, et al. The assessment of antiangiogenic and antivascular therapies in early-stage clinical trials using magnetic resonance imaging: issues and recommendations. Br J Cancer 2005;92:1599–610.
11. Cenic A, Nabavi DG, Craen RA, et al. A CT method to measure hemodynamics in brain tumors: validation and application of cerebral blood flow maps. AJNR Am J Neuroradiol 2000;21:462–70.
12. Roberts HC, Roberts TP, Lee TY, et al. Dynamic contrast-enhanced computed tomography (CT) for quantitative estimation of microvascular permeability in human brain tumors. Acad Radiol 2002;9:Suppl 2: S364–7.
13. Roberts HC, Roberts TP, Lee TY, et al. Dynamic, contrast-enhanced CT of human brain tumors: quantitative assessment of blood volume, blood flow, and microvascular permeability: report of two cases. AJNR Am J Neuroradiol 2002;23:828–32.
14. Gobbel GT, Cann CE, Fike JR. Measurement of regional cerebral blood flow using ultrafast computed tomography. Theoretical aspects. Stroke 1991;22:768–71.
15. Law M, Young R, Babb J, et al. Comparing perfusion metrics obtained from a single compartment versus pharmacokinetic modeling methods using dynamic susceptibility contrast-enhanced perfusion MR imaging with glioma grade. AJNR Am J Neuroradiol 2006;27:1975–82.
16. Toennis W, Walter W. [Glioblastoma multiforme (report on 2611 cases).] Acta Neurochir Suppl (Wien) 1959;6:40–62.
17. Kleihues P, Louis DN, Scheithauer BW, et al. The WHO classification of tumors of the nervous system. J Neuropathol Exp Neurol 2002; 61:215–25.
18. Wiest R, Bredow F von, Schindler K, et al. Detection of regional blood perfusion changes in epileptic seizures with dynamic brain perfusion CT – a pilot study. Epilepsy Res 2006;72:102–10.
19. Meier P, Zierler KL. On the theory of the indicator-dilution method for measurement of blood flow and volume. J Appl Physiol 1954;6:731–44.

20. Ostergaard L, Sorensen AG, Kwong KK, et al. High resolution measurement of cerebral blood flow using intravascular tracer bolus passages. Part II: Experimental comparison and preliminary results. Magn Reson Med 1996;36:726–36.
21. Bozzao A, Fasoli F, Finocchi V, et al. Long term evaluation of brain perfusion with magnetic resonance in high flow extracranial-intracranial saphenous graft bypass. Eur Radiol 2007;17:33–8.
22. Caramia F, Santoro A, Pantano P, et al. Cerebral hemodynamics on MR perfusion images before and after bypass surgery in patients with giant intracranial aneurysms. AJNR Am J Neuroradiol 2001;22:1704–10.
23. Greitz T, Cronqvist S. Angiographic evaluation of cerebral circulation time and regional cerebral blood flow. A comparative study. Scand J Clin Lab Invest Suppl 1968;102:XI.
24. Calli C, Kitis O, Yunten N, et al. Perfusion and diffusion MR imaging in enhancing malignant cerebral tumors. Eur J Radiol 2006;58:394–403.
25. Eastwood JD, Provenzale JM. Cerebral blood flow, blood volume, and vascular permeability of cerebral glioma assessed with dynamic CT perfusion imaging. Neuroradiology 2003;45:373–6.
26. Lee SJ, Kim JH, Kim YM, et al. Perfusion MR imaging in gliomas: comparison with histologic tumor grade. Korean J Radiol 2001;2:1–7.
27. Aronen HJ, Glass J, Pardo FS, et al. Echo-planar MR cerebral blood volume mapping of gliomas. Clinical utility. Acta Radiol 1995;36:520–8.
28. Aronen HJ, Pardo FS, Kennedy DN, et al. High microvascular blood volume is associated with high glucose uptake and tumor angiogenesis in human gliomas. Clin Cancer Res 2000;6:2189–200.
29. Knopp EA, Cha S, Johnson G, et al. Glial neoplasms: dynamic contrast-enhanced T2*-weighted MR imaging. Radiology 1999;211:791–8.
30. Lin TN, Sun SW, Cheung WM, et al. Dynamic changes in cerebral blood flow and angiogenesis after transient focal cerebral ischemia in rats. Evaluation with serial magnetic resonance imaging. Stroke 2002; 33:2985–91.
31. Cronqvist S, Greitz T. Cerebral circulation time and cerebral blood flow. Acta Radiol Diagn 1969;8:296–304.
32. Kiselev VG. On the theoretical basis of perfusion measurements by dynamic susceptibility contrast MRI. Magn Reson Med 2001;46:1113–22.
33. Greitz T. Normal cerebral circulation time as determined by carotid angiography with sodium and methylglucamine diatrizoate (Urografin). Acta Radiol Diagn 1968;7:331–6.
34. Mihara F. Reliability of mean transit time obtained using perfusion-weighted MR imaging; comparison with positron emission tomography. Magn Reson Imaging 2003;21:33–9.
35. Mariani L, Schroth G, Wielepp JP, et al. Intratumoral arteriovenous shunting in malignant gliomas. Neurosurgery 2001;48:353–7.
36. Ellika SK, Jain R, Patel SC, et al. Role of perfusion CT in glioma grading and comparison with conventional MR imaging features. AJNR Am J Neuroradiol 2007;28:1981–7.

Address for Correspondence
PD Dr. Christoph Ozdoba
Institute of Diagnostic and Interventional Neuroradiology
Inselspital
University of Bern
3010 Bern
Switzerland
Phone (+41/31) 632-2655, Fax -4872
e-mail: christoph.ozdoba@insel.ch